Available online at www.sciencedirect.com

ScienceDirect

Structural Integrity Procedia 00 (2025) 000–000

Structural Integrity Procedia

www.elsevier.com/locate/procedia

XX ANIDIS Conference

Shake table testing of a pre and post-retrofitted unreinforced masonry structure: Preliminary experimental and numerical results

Fabio Di Trapani[a]*, Sofia Villar[b], Marilisa Di Benedetto[b], Alessandra Marini[c], Chiara Passoni[c], Andrea Belleri[c], Giacomo Navarra[d], Francesco Lo Iacono[d], Maria Oliva[d], Marinella Fossetti[d], Giuseppe D'Arenzo[d], Denise Li Cavoli[d], Davide Campanini[e], Guido Camata[f], Enrico Spacone[f]

[a]*Università degli Studi Di Palermo, Dipartimento di Ingegneria, Viale delle Scienze Ed. 8, 91128, Palermo, Italy*
[b]*Politecnico di Torino, Dipartimento di Ingegneria Strutturale, Edile e Geotecnica, Corso Duca degli Abruzzi 24, 10129, Turin, Italy*
[c]*Università degli Studi di Bergamo, Dipartimento di Ingegneria e scienze applicate, Via Salvecchio 19 24129, Bergamo, Italy*
[d]*Università degli Studi di Enna Kore, Dipartimento di Ingegneria e Architettura, Enna, 94100, Italy*
[e]*Kerakoll Spa, Via dell'Artigianato 9, 41049, Sassuolo, Italy*
[f]*Università degli Studi "G. D'Annunzio" Chieti-Pescara, Dipartimento di Ingegneria e Geologia, Viale Pindaro 42, Pescara, Italy*

Abstract

The paper presents the results of an experimental campaign on a ¾-scaled unreinforced masonry structure subjected to bidirectional shaking table tests carried out at the L.E.D.A. Laboratory of the Kore University of Enna. The study investigates the impact of progressive retrofitting and repair strategies for the as-built structure, which was designed to represent a heritage residential building of central Italy. Three sequential shaking table tests were carried out. In the first test, the as-built configuration was tested up to the early damage achievement. In the second test, prior stiffening and strengthening of the floor slabs was performed, also including improved connections of the floor slabs with the perimeter walls. For the third test, the structure was repaired by the application of internal and external FRCM layers to the masonry walls. A detailed 3D finite element model of the three configurations of the specimen was developed with the STKO software platform for OpenSees to reproduce the experimental tests and complement the interpretation of the experimental results. The preliminary results shown in the paper illustrate the influence of the progressively introduced retrofit interventions by assessing structural performance in terms of damage onset and propagation, and capability of the retrofitting systems in repairing prior seismic damage.

Peer-review under responsibility of XX ANIDIS Conference organizers
Keywords: Masonry, Retrofitting, FRCM, Finite Element, Shaking Table, OpenSees, STKO.

* Corresponding author.
E-mail address: fabio.ditrapani@unipa.it

1. Introduction

In Italy, as well as across the broader Mediterranean region, a large portion of the existing building stock consists of unreinforced masonry (URM) structures. Despite their historical and cultural value, these structures have highlighted significant vulnerability to seismic events, mainly because of their low ductility, insufficient structural connections and lack of structural regularity. The extensive damage and losses observed during recent earthquakes, such as the 2009 L'Aquila earthquake, the 2012 Emilia earthquake, and the 2016 central Italy seismic sequence, including Amatrice earthquake, have underscored the urgent need for effective seismic assessment and retrofitting strategies to protect both human lives and cultural heritage (D'Ayala and Paganoni 2011, Penna et al. 2012, Acito et al. 2021). Nowadays significant advancements have been made in seismic retrofitting and repair techniques for URM structures to provide additional resistance to the walls (e.g., grout injections, reinforced plasters, fiber-reinforced polymers (FRP) and fiber-reinforced cementitious matrix (FRCM)) as described by Corbi 2013, Sandoli et al. 2020, Alecci et al. 2024. Other typologies of interventions, such as external or internal perimeter curbs, floor-to-wall connections and tie are commonly used to limit the local out-of-plane mechanisms often occurring during major earthquakes. In addition, floor stiffening intervention are often performed to reduce wooden floors deformability and enhance the distribution of seismic forces to be proportional to the bearing walls' stiffness. Despite this large catalogue of interventions, that have been proved to be effective at local level, their real effectiveness at the global level remains limited (Sasthiparan et al. 2014, Ruiz et al. 2023, Qiyun et al. 2025). Alongside experimental testing, numerical simulations have become an indispensable counterpart, allowing the extrapolation of additional information as well as the simulation of supplementary numerical tests (Di Trapani et al. 2024a, 2024c, Tomić and Beyer 2024, Di Trapani et al. 2025).

In this framework, this paper presents the preliminary results of a shake table experimental campaign carried out at the L.E.D.A. Laboratory (Fossetti et al. 2017) of the Kore University of Enna (Italy). The tests are be conducted on a ¾-scale, two-story masonry specimen representative of typical heritage buildings in central Italy. The specimen is made of solid brick masonry and wooden floors, and it has been tested with three configurations: a) as-built configuration; b) improved floor stiffness and floor-to-wall connections; and c) and doble-side FRCM reinforcement of the walls. The specimen was equipped with triaxial accelerometers at the relevant points of each storey. Refined three-dimensional finite element models of the structure in the different configurations were developed using the STKO platform for OpenSees to complement the investigation. The preliminary results showed the effectiveness of the incremental retrofitting interventions in terms of modification of the dynamic response and cracking patterns.

2. Specimen details and retrofitting configurations

The specimen replicates a typical small-scale masonry building made of solid brick masonry walls and timber floors. The structure is two stories high, consisting of four orthogonal walls forming a rectangular plan measuring 3.0 m × 4.0 m, with a total height of 5.75 m. The wall thickness is 25 cm. The design drawings of the specimen are illustrated in Fig. 1. An outer view of the specimen is shown in Figs. 2a and 2b. The brick masonry texture can be observed from Fig. 1c as well as the assembly of the wooden roof.

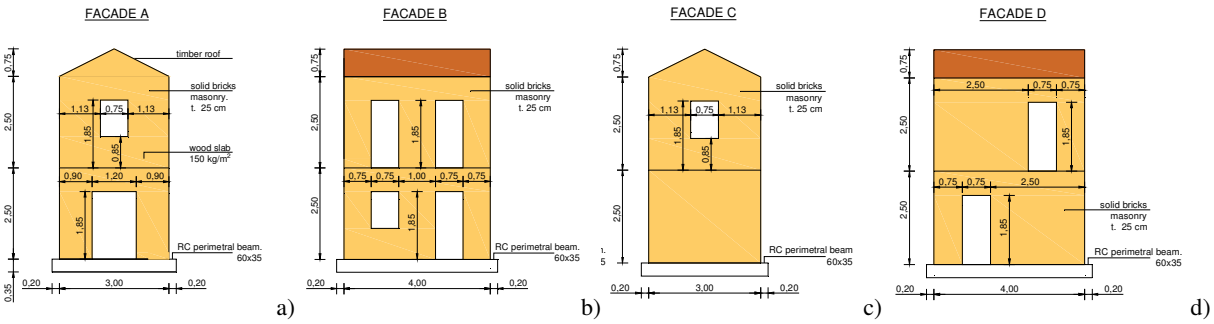

Fig. 1. Design drawings of the specimen facades: a) facade A; b) facade B, c) facade C, d) facade D.

The specimen was designed to observe both in-plane and out-of-plane damage mechanisms during testing and the effect of structural irregularity. For this purpose, asymmetrical and vertically misaligned openings were introduced (Fig. 1, 2). At the first storey the floor slab is made of seven rectangular wooden beams (12 × 14 cm), evenly spaced along the longitudinal direction. The double-pitched timber roof comprises seven wooden beams (12 × 10 cm) connected to a simply supported ridge beam (14 × 20 cm) (Fig. 1c). A 25 mm wooden plank system is connected to the main beams. The planks are not connected one to each other, so in the as-built configuration the deformable floor hypothesis takes place. The specimen was built on a 60 × 35 cm reinforced concrete foundation beam, which is anchored to the shaking table. The connection between the foundation and the masonry walls was ensured by Ø16 mm rebars, spaced at 50 cm intervals, to prevent relative displacement between the foundation beam and the specimen during the tests. The masonry was arranged with solid clay bricks (12 × 25 × 150 mm) having an average compressive strength f_{bm}=15.18 MPa combined with a natural hydraulic lime (NHL 3.5), with an average strength of f_{mm}=6.7 MPa. The bricks were placed with the longer dimensions orthogonal to the perimeter of the specimen with a "double head" laying scheme. The resulting average compressive and shear strength of the masonry were 8.2 MPa and 0.25 MPa respectively. The design permanent loads for the specimens were 1.5 kN/m^2 for the 1st storey and 0.40 kN/m^2 for the 2nd storey. The design live loads obtained by using the combination factor according to the Italian NTC 2018 were 2.0 x 0.3=0.6 kN/m^2 for the 1st storey and no live loads for the 2nd storey.

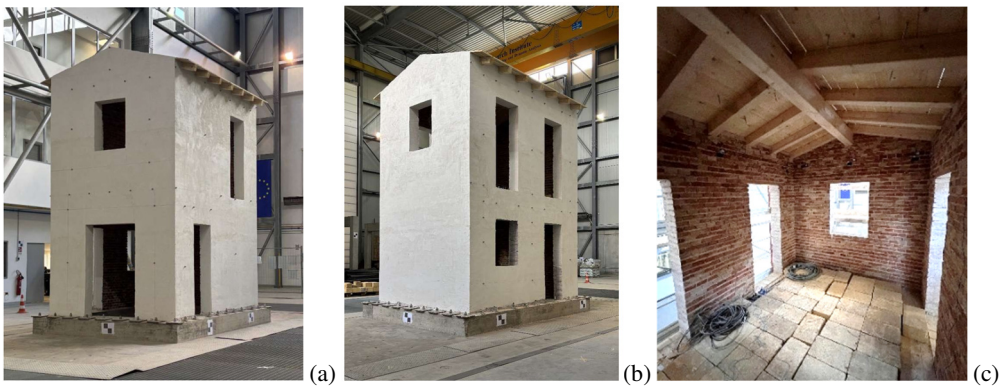

(a) (b) (c)

Fig. 2. Views of the specimen: a) outer view of facades A and B; b) outer view of facades C and D; c) inner view of the specimen at the first floor.

2.1. Case study tests

The shake table tests were carried out for three different configurations referred to as:

- As-built configuration (AB)
- Enhanced floor stiffness and connection (EFS)
- Enhanced floor stiffness and connection + FRCM Retrofitted Walls (EFS+RW)

The as-built configuration represents the above-described existing masonry structure with deformable floors and is firstly subjected to shake table tests of increasing intensity up to the achievement of early damage. The EFS configuration was arranged on the same (previously damaged) specimen. The tests provided increased earthquake amplitudes up to the severe damage limit state. The floor stiffness was enhanced to provide a diaphragm like behaviour of the slabs. A Kerakoll ® retrofit system was used consisting of a thin 30 mm fiber reinforced cementitious (FRC) mortar (Geolite Magma Xenon) layer (Fig. 3a). The concrete topping slab was structurally connected to the timber floor through metal shear connectors screwed into the wooden planks. Additionally, the floor has been tied to the perimeter masonry walls by means of stainless-steel connectors, which are anchored into the masonry and embedded within the slab. Finally, the EFS+RW configuration was arranged on the severely damaged specimen as a repair and retrofit strategy. FRCM (Geocalce F Antisismico) reinforcement with a basalt (Geosteel Grid 200) fiber grid was provided for the masonry walls inner and outer sides. The reinforcement layers were connected by stainless-steel traverse connectors (Fig. 3b, 3c).

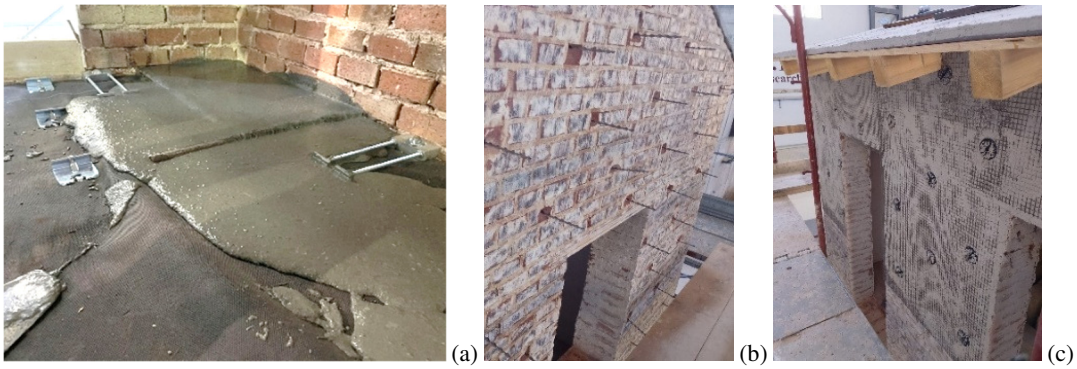

Fig. 2. Views of the retrofitting phases: (a) EFS configuration, concrete cast and views of connectors; (b) EFS+RW configuration, arrangement of the transverse stainless dowels; (c) EFS+RW configuration, arrangement of the first FRCM mortar layer and basalt grid.

3. Test setup, instrumentation and input

The specimen was arranged over the L.E.D.A. Laboratory six-degree of freedom shake table having 4.0 x 10.0 m dimensions in plan. The accelerations of the shaking table were measured using sixteen single-axis MEMS accelerometers, positioned on the shaking table at the spherical joint on top of each of the horizontal and vertical hydraulic actuators (4 in the X direction, 4 in the Y direction, and 8 in the Z direction). 24 accelerometers were installed in the specimen in the positions indicated in Fig. 3. It is worth noting that the sensors were installed on the internal sides of the walls of the building and oriented so that their axes were aligned with those of the global reference system (Fig. 4a). Due to the absence of floor tie beams, it was assumed that, at least in the initial test configuration, each wall could undergo displacements independently of the others. Therefore, on each of the four elevations and for each story level, two biaxial accelerometers (measuring only the horizontal components) were placed at the endpoints of the elevation. In addition, a single-axis accelerometer was positioned at the mid-span of the wall to measure the out-of-plane acceleration component. An overall view of the specimen in the shake table is shown in Fig. 4b. To simulate the permanent design and live loads additional masses of 1848 kg and 361 kg were added to the first storey and the roof. The reference ground motion input consisted of two horizontal components of the AQG record from Colle Grilli (L'Aquila, Italy, April 6, 2009) which were applied to the x and y components. The response spectra of the two components of the ground motion are depicted in Fig. 4c. The sequence of the tests for each configuration is illustrated in Table 1.

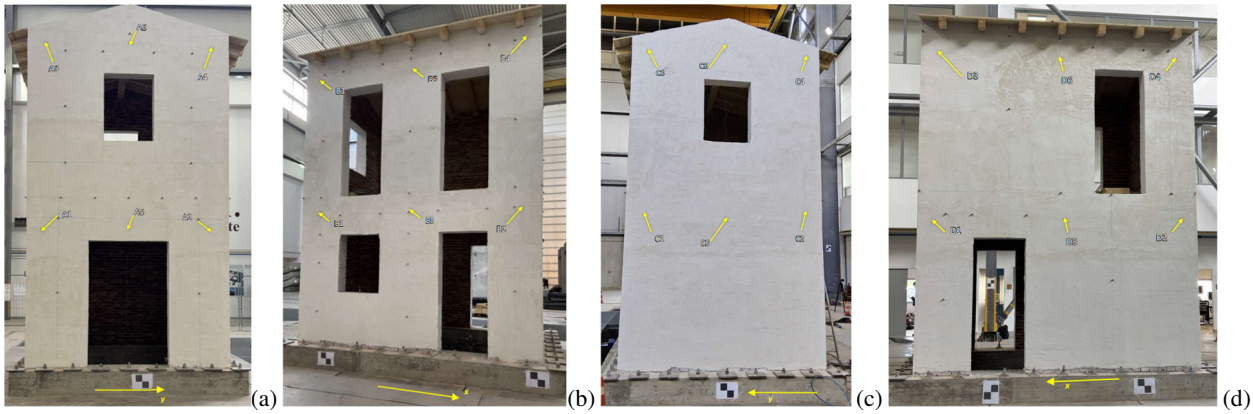

Fig. 3. Position of the accelerometers: (a) Façade A; (b) Façade B; (c) Façade C; (d) Façade D.

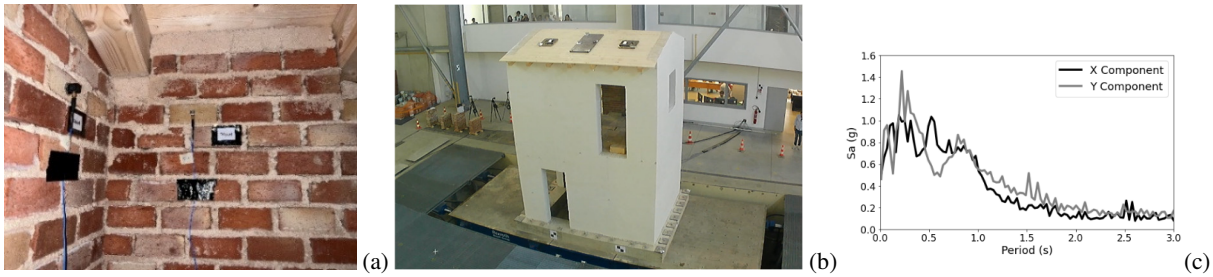

(a) (b) (c)

Fig. 4. (a) View of the sensors installed in the inner sides of the walls; (b) Overall view of the specimen in the shake table; (b) Response spectra of the reference input earthquakes.

Table 1. Shake table test sequences.

Configuration	Percentage intensity with respect to the reference GM												
AB	5%	10%	20%	30%	40%	50%	60%	70%	80%	90%			
EFS						50%		70%		90%	110%		
EFS+RW						50%		70%		90%	110%	120%	130%

4. Test results from damage evolution and frequency output

4.1. AB Configuration

Ten tests were carried out up to 90% of the intensity of the reference ground motion. The first test was performed with a 5% intensity. The intensity gradually increased to match an early damage (damage limitation) limit state where the specimen was not compromised and so the subsequent slab reinforcement could be performed without the need for significant repair interventions to the walls. The first cracks were observed at 80% intensity. They involved the masonry piers at the ground storey of façade A (Fig. 5a). The crack occurred horizontally at the top of the piers denoting a flexural mechanism. In the subsequent shaking (90%) the same cracks advanced. The corner pier between façades A and B separated from the upper storey due to the complete extension of the horizonal crack (Fig. 6a).

4.2. EFS Configuration

The specimen with the retrofitted slab did not experience damage increments up to 90%. The severe damage limit state was achieved at the last shaking 110% intensity. The cracks mainly started from the corners of the openings and propagated in the connection regions at the floor level (Fig. 5b). Horizonal flexural cracks were also observed at the top of the first storey piers. Façade B central pier at the 1st storey also showed compression failure at the top cross section due to the flexural action. A large shear crack occurred at the ground storey solid wall in Façade C. This can be interpreted as the consequence of the effectiveness of the reinforced slab in distributing seismic forces proportionally to the walls stiffness, limiting the irregular major demand to the less stiff façades A and B.

4.3. EFS+RW Configuration

The specimen was fully retrofitted with double FRCM layers. Some local repairs were carried through inclined stainless bars to reconnect the portion of masonry that failed in compression. The tests were carried out starting from 50% intensity and up to 130%. Despite the severe prior damage, the retrofitted specimen did not experience damage at 50% and 70% intensities. Limited crack re-opening was observed at 90% in correspondence of the slender ground storey piers in façade A and at the corner with façade B. In the subsequent shaking (110%) the previous cracking pattern experienced in the EFS configuration reappeared, but the cracks had a lower extent due to the presence of the activation of the basalt grid (Fig. 5c). In the two other shakings (120% and 130%) no significant new cracks opened. A moderate increase in the extent of the cracking pattern was observed, mostly as localized damage to the FRCM

mortar layer in correspondence with the masonry cracks. However, the local exposure of the basalt grid did not reduce its effectiveness in providing additional tensile strength, as it remained effectively bonded in the adjacent areas. The overall mechanism was characterized by a controlled crack opening and closure. No increments of the shakings were given to prevent the risk of global instability of the specimen.

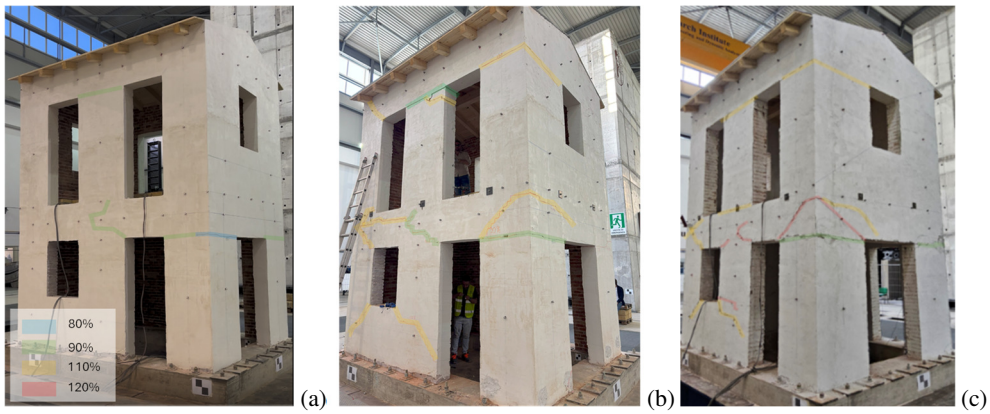

Fig. 5. Crack patterns at the end of the sequential shakings: (a) AB; (b) EFS; (c) EFS+RW

4.4. Frequency response

Before and at the end of each test, noise measurements were carried out by applying low-intensity excitations separately in the *x* and *y* directions. The transfer functions *H(f)* obtained from two sensors at two parallel walls are illustrated in Fig. 6. For the sake of space only the results in *y* direction are illustrated in Fig. 6. The as-built specimen has a clear dominant frequency of 7.3 Hz (T=0.137 s). A 0.5 Hz decay was observed at the end of the first sequence of shakings. The final frequency was 6.8 Hz. For the EFS specimen, the slab retrofitting did not show significant stiffness recovery, having an initial frequency of 6.9 Hz. After the 110% intensity tests a relevant stiffness decay to 5.8 Hz was observed, highlighting a clear correlation with the severe damage experienced by the specimen. The before-test frequency of the EFS+RW specimen was 6.8 Hz, demonstrating that the full retrofit of the walls with the FRCM system was effective to recover the initial stiffness. After the 130% intensity shaking the EFS+RW specimen main frequency decayed to 5.9 Hz, which is close to that of the EFS specimen after the 110% intensity shaking.

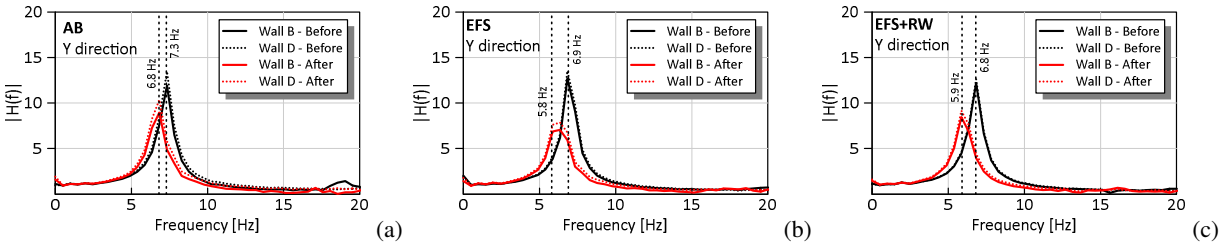

Fig. 6. Transfer function at the beginning and at the end of the sequential shakings: (a) AB; (b) EFS; (c) EFS+RW

5. Numerical model and preliminary simulation of the tests

Preliminary numerical models of the specimens were developed using the STKO (Petracca et al 2017) software platform for OpenSees. Masonry walls were modelled using the homogenized masonry approach with layered elements as also proposed by Di Trapani et al 2024b. The layered shell formulation allows multiple material layers across the thickness, making it suitable to reproduce retrofitted configurations. A mesh size of 200 mm was adopted, providing a suitable balance between computational efficiency and accuracy. A scheme of the model is illustrated in Fig. 7a. The constitutive model for the homogenized masonry was defined using the ASDConcrete3D material

(Petracca et al. 2022) which characterizes both tensile and compressive damage-plasticity behavior. Lintels above the openings were explicitly modelled with a surrounding mortar band represented to reproduce the cohesive–frictional behavior. For the beams 1D elastic elements were used. In the EFS and EFS+RW configuration, the floor plate was modelled as a layered shell element combining the slab planks and the FRC layer. To account for the decoupling between shear modulus (G) and Young's modulus (E) of the slab the orthotropic Material Wrapper was applied. The simulation of the FRCM layers was carried out by adding two extra layers per side to the shells. Each extra-layer reproduces the 1D response of the fiber in one direction. The layer overlapping allows to consider the responses of the FRCM in the two orthogonal directions. For the FRCM a linear elastic material model with elastic Young's modulus E=62000 MPa and a strength limit of 1100 MPa was adopted.

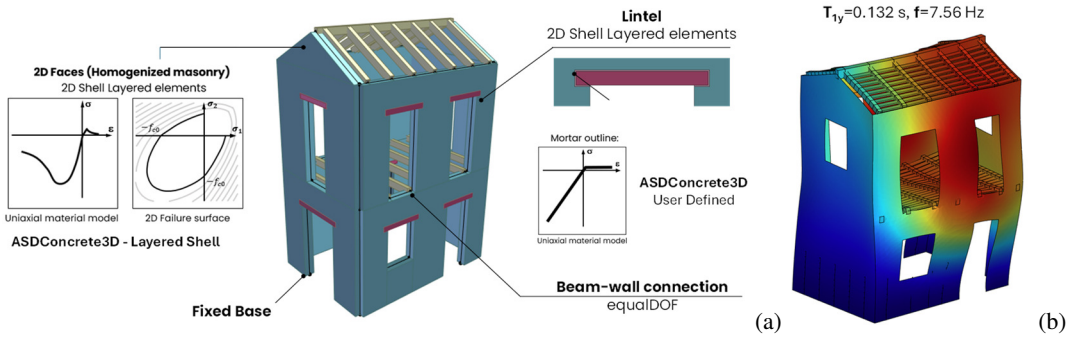

Fig. 7. (a) Numerical model assembly scheme with STKO; (b) First numerical modal shape in y direction.

An elastic calibration of the model was carried out with the AB configuration by comparing the experimentally detected main frequencies and the numerical ones. For the sake of space only the modals shape of the main vibration mode in *y* is shown in Fig. 7b. The numerically detected frequency (7.56 Hz) aligns with the experimental one (7.3 Hz). The modal shape shows an irregular response with the tendency to a major displacement of façade A.

Preliminary simulations of the tests were carried out and the damage patterns at the end of the tests are compared in Fig. 8. It can be observed that most of the main crack patterns were effectively captured by the proposed model formulation. Same discrepancies can be justified by the use of the homogenized masonry formulation that can be less performative in revealing flexural cracks at the very weak mortar joints for lowest intensities. In addition, these tests were performed with the final shaking intensity and therefore they are not considering the prior damage accumulation. Despite its simplicity and computational efficiency, the proposed modelling strategy produces promising results, although additional refinement is necessary to improve its representativeness.

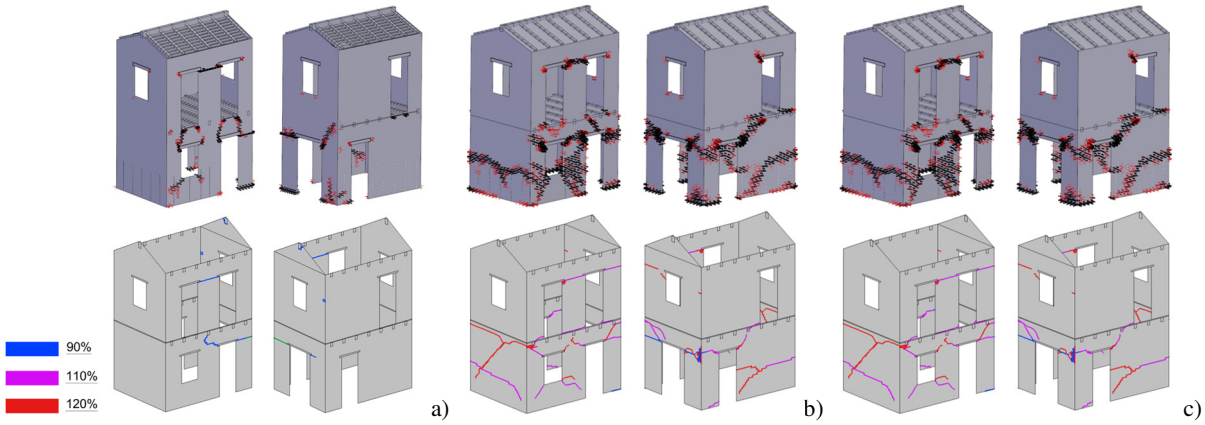

Fig. 8. Numerical vs. experimental comparison at the end of the tests: (a) AB model 90%; (b) EFS model 110%; (c) EFS+RW model 130%.

6. Conclusions

This study presented an experimental and numerical investigation on a ¾-scale unreinforced masonry building subjected to bidirectional shake table tests under progressive retrofitting and repair strategies. The results showed that floor stiffening and improved floor-to-wall connections (EFS) enhanced seismic resistance and delayed the onset of severe damage compared to the as-built configuration, while the application of double-sided FRCM reinforcement to the walls (EFS+RW) effectively restored the initial stiffness and controlled crack development even under high-intensity shaking. The observed decay in fundamental frequency correlated well with damage progression, confirming its reliability as a simple indicator of structural degradation. Numerical simulations based on a homogenized masonry FE model reproduced the main experimental trends and damage patterns, although further refinement is needed to improve representativeness. Overall, the findings demonstrate that combined floor and wall retrofitting strategies can restore and even enhance the performance of previously damaged URM buildings.

Acknowledgements

This study was funded by the Project **GENESIS**: Seismic risk management for the touristic valorization of the historical centres of Southern Italy. PON MIUR “Re-search and Innovation” 2014 - 2020 and FSC. D.D. 13/07/2017 n. 1735. The authors also thank **Kerakoll®** company for sponsoring the reinforcement of the specimen.

References

D’Ayala, F., Paganoni, S. (2011). Assessment and analysis of damage in L’Aquila historic city centre after 6th April 2009. Bull. Earthq. Eng., 9, 81–104.

Penna, A., Morandi, P., Rota, M., Manzini, C.F., da Porto, F., Magenes, G. (2014). Performance of masonry buildings during the Emilia 2012 earthquake. Bull. Earthq. Eng., 12, 2255–2273.

Acito, M., Garofane, M.S., Magrinelli, E., Milani, G. (2021). The 2016 Central Italy seismic sequence: Linear and non-linear interpretation models for damage evolution in S. Agostino’s church in Amatrice. Bull. Earthq. Eng., 19, 1467–1507.

Alecci, V., Fagone, M., Galassi, S., Rotunno, T., Stipo, G., De Stefano, M. (2024). Experimental shear behaviour of masonry walls reinforced with FRCM. Constr. Build. Mater., 315, 118425.

Corbi, I. (2013). FRP reinforcement of masonry panels by means of C-fiber strips. Compos. B Eng., 47, 348–356.

Sandoli, A., Pacella, G., Lignola, G.P., Calderoni, B., Prota, A. (2020). FRP-reinforced masonry spandrels: Experimental campaign on reduced-scale specimens. Constr. Build. Mater., 261, 119965.

Qiyun, Q., Jia, P., Wenchao, L., Wanlin, C., Jing, Y., Hu, X. (2025). Shaking table tests on masonry structures retrofitted with steel-polymer mortar after earthquake damage. Eng. Struct., 330, 119866.

Ruiz, D.M., Barrera, N., Reyes, J.C., et al. (2023). Bi-axial shaking table tests to evaluate the seismic performance of two-story rammed-earth walls retrofitted with steel plates. Bull. Earthq. Eng., 21, 6393–6422.

Sathiparan, N., Sakurai, K., Numada, M., Meguro, K. (2014). Seismic evaluation of earthquake resistance and retrofitting measures for two-story masonry houses. Bull. Earthq. Eng., 12, 1805–1826.

Di Trapani, F., Oddo, M.C., Sberna, A.P., La Mendola, L. (2024a). Structural health monitoring of masonry structures using stress sensors: Experimental induced damage tests and proposed approach for real-time monitoring. Constr. Build. Mater., 449, 138077.

Di Trapani, F., Di Benedetto, M., Sberna, A.P., Camata, G. (2025). Local shear demand correction model for the analysis of infilled frames using equivalent struts. J. Struct. Eng.. https://doi.org/10.1061/JSENDH/STENG-14684

Tomić, I., Beyer, K. (2024). Shake-table test on a historical masonry aggregate: Prediction and postdiction using an equivalent-frame model. Bull. Earthq. Eng., 22, 6225–6258.

Di Trapani, F., Di Benedetto, M., Petracca, M., Camata, G. (2024c). Local infill-frame interaction under seismic loads: Investigation through refined micro-modelling. Eng. Struct., 315, 118088.

Di Trapani, F., Villar, S., Di Benedetto, M., Petracca, M., Camata, G. (2024b). Seismic response of unreinforced masonry building aggregates: Investigation on the “aggregate effect” based on an elementary building aggregate. Eng. Struct., 316, 118301.

Fossetti, M., Lo Iacono, F., Minafò, G., Navarra, G., Tesoriere, G. (2017). A new large scale laboratory: the LEDA research centre (Laboratory of Earthquake engineering and Dynamic Analysis), in: Int. Conf. Adv. Exp. Struct. Eng., 2017. https://doi.org/10.7414/7aese.T6.18.

Ministerial Decree 17/01/2018 (NTC 2018). Aggiornamento delle norme tecniche per le costruzioni. Ministry of Infrastructures and Transportation, Italy.

Petracca, M., Candeloro, F., Camata, G. (2017). ASDEA Software STKO user manual. ASDEA Software Technology.

McKenna, F., Fenves, G.L., Scott, M.H. (2000). Open system for earthquake engineering simulation. University of California, Berkeley, CA.

Petracca, M., Camata, G., Spacone, E., Pelà, L. (2022). Efficient constitutive model for continuous micro-modelling of masonry structures. Int. J. Archit. Herit., 17, 1–13.